Electronic properties of boron nitride nanocones under the influence of parallel and perpendicular external electric fields

D. Pedreira, S. Azevedo, and M. Machado
Departamento de Física, Universidade Estadual de Feira de Santana, Feira de Santana, Bahia, Brazil
(Received 30 May 2008; revised manuscript received 28 July 2008; published 22 August 2008)

Boron-nitride nanocones with 60°, 120°, and 240° disclination under the influence of parallel and perpendicular external electric fields are studied through first-principles calculations based on the density-functional theory. It is shown that the application of the external electric field ranging from 0 to 0.5 $V/Å^{-1}$, either parallel or perpendicular to the cones' axis, does not change significantly the formation energy of those systems. Changes at the densities of states according to the direction of the applied electric field are also analyzed showing that, except for the 240° cone, the perpendicular field is more effective for gap reduction of those structures. A second-order Stark effect, more pronounced for the perpendicular direction, is observed when the energy shift is analyzed for the cones under the influence of the electric fields.

DOI: 10.1103/PhysRevB.78.085427 PACS number(s): 73.22.−f, 71.20.Tx, 71.15.Mb

I. INTRODUCTION

Curved nanostructures, carbon fullerenes and nanotubes being the most known examples, have been the focus of increasing scientific and technological interest due to their unique electronic and mechanical properties.[1–3] Carbon nanocones were observed for the first time in 1992 as caps at the ends of nanotubes,[4] and as free-standing structures two years later.[5,6] Nanocones are interesting materials for technological application since they present a particular structure with a sharp tip which leads to specific electronic and mechanical properties. Several ideas for using those structures as electronic devices have emerged, in fact carbon nanocones have been studied as cold field-emission electron sources recently.[7,8] Boron-nitride (BN) nanostructures are, however, more appealing than their carbon counterparts since they are known to present chemical oxidation inertness and mechanical toughness.[9,10] As a novel form of BN nanostructures, BN nanocones are promising cold electron sources in field-emission devices and their possible application will depend on the particular structure of their tips and on their behavior under electric fields.

Cones are characterized according to their disclination angle D_θ that is defined as the angle of the sector removed from a flat sheet to form a cone. For carbon nanocones we have only five disclination angles which satisfy the continuity condition at the junction of the flat graphene sheet (D_θ =60°,120°,180°,240°, and 300°) and only C–C bonds, while for the BN ones we can observe three types of covalent bonds, that are B–N, B–B, and N–N, which lead to differences in physical, chemical, and electronic properties between carbon and boron-nitride nanostructures.[11–14] BN nanostructures such as nanocages, nanohorns, nanorods, single-walled and multiwalled nanotubes, and nanocones with disclination angles of 120°, 240°, and 300° have been synthesized in laboratories[13–17] and the field-emission current from those systems has been experimentally observed at low voltage.[18] Also it was shown that a perpendicular electric field applied to BN nanotubes can tune the electric properties of those tubes.[19] Several studies for external electric fields applied alongside cones' axis of BN nanocones have been done already,[20–23] however, there is no report of any results for a field perpendicularly applied to those structures so far. In this sense we have made a complete study for three BN nanocone structures, namely, 60°, 120°, and 240°, under the influence of parallel and perpendicular external electric fields with varying magnitudes, with the analysis of the formation energy, densities of states, energy shift, and electronic density of these structures.

II. METHODOLOGY

The studied cones with 60°, 120°, and 240° disclination are shown in Fig. 1. The cone with 60° is characterized for having a pentagonal ring at its apex and for presenting a line of defects at its wall that can be formed either by B–B [Fig. 1(a)] or N–N [Fig. 1(b)] homonuclear bonds, with 59 boron (B) and 56 nitrogen (N) atoms for the first case and 56 B and 59 N atoms for the second one. The cone with 120° disclination presents a square ring at its apex, B–N bonds only [Fig. 1(c)] and is composed by 46 B and 46 N atoms. Finally, the nanocone with 240° disclination, formed by 62 B and 62 N atoms, is characterized for having an apex composed by two atoms (one B and one N) at the top of one unusual hexagonal ring that is bifurcated at its bottom part and is located at the tip of the cone [Fig. 1(d)]. All the cones are saturated with hydrogen (H) atoms at their open edges. The external electric field is applied in two different directions, parallel and perpendicular to cones' axis with magnitudes ranging from 0 to 0.5 $V/Å$.

All the calculations were done through the density-functional theory[24] with the treatment of exchange and correlation functional by the generalized gradient approximation parametrized by Perdew *et al.*,[25] as implemented in SIESTA code.[26] A linear combination of pseudoatomic[27,28] double zeta quality basis set, with polarization functions, is used. The interaction between the ionic cores and the valence electrons is represented by norm-conserving Troullier-Martins pseudopotentials[29] in the Kleinman-Bylander factorized form.[30] Self-consistent field calculations were done with a convergence criterion of 10^{-4} eV on the total energy and electron density. The employed supercell is a box with di-

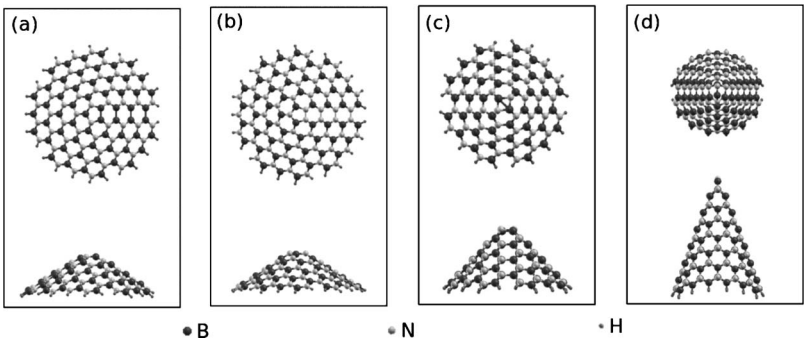

FIG. 1. Top and lateral pictorial schemes of studied cones with (a) 60° B–B, (b) 60° N–N, (c) 120°, and (d) 240° disclination.

mensions equal to $35\times35\times20$ Å^3, for the cones with 60° and 120° disclination, and $35\times35\times40$ Å^3 , for the 240° one, which is large enough to exclude interactions between cones in adjacent cells and to avoid the presence of electric charges near the cell boundaries. The largest cone dimension along the cone axis is around 14 Å, while the largest diameter is 17 Å approximately. A fully optimization of all atomic positions was realized until atomic forces were less than 0.1 eV/Å.

III. RESULTS AND DISCUSSION

Through the analysis of the formation energy of the cones, 120° and 240° is possible to compare the stability of those systems which are interesting since they do not present homonuclear bonds like the one with 60° disclination. Besides, the number of B and N atoms and the number of B–H and N–H bonds is the same for each nanocone (46 B and 46 N for the 120° and 62 B and 62 N for the 240° one). The formation energy is given by:

$$E_f = E_T - n_B\mu_B - n_N\mu_N - n_{BH}\mu_{BH} - n_{NH}\mu_{NH}, \quad (1)$$

where E_T is the total energy, n_B is the number of B atoms, n_N is the number of N atoms, n_{BH} is the number of B–H bonds, n_{NH} is the number of N–H bonds, and the chemical potentials are μ_B, μ_N, μ_{BH}, and μ_{NH}, respectively. Since $n_B=n_N$, $n_{BH}=n_{NH}$, $\mu_B+\mu_N=\mu_{BN}$, and $\mu_H=\frac{1}{2}(\mu_{NH}+\mu_{BH})$, for each system, Eq. (1) can be written as

$$E_f = E_T - n_{BN}\mu_{BN} - n_H\mu_H, \quad (2)$$

where n_H is the number of H atoms, n_{BN} is the number of BN pairs, and prior determination of the chemical potentials.[12] As can be seen in Table I, the external electric field has little influence at the stability of analyzed structures. We can also see that the 240° disclination cone presents a higher value for the formation energy, even without the presence of the external electric field. This can be associated with the higher curvature and consequently the higher energy strain associated with the 240° cone when compared to the others.

For the densities of states we have made a comparison of the external electric field influence, parallel and perpendicular to the cones' axis, with magnitudes equal to 0, 0.3, and 0.5 V/Å, respectively. At Fig. 2 we have the densities of states for the cones with (a) 60° B–B, (b) 60° N–N, (c) 120°, and (d) 240° disclination. The left column (a_1, b_1, c_1, and d_1) is composed by the cones under the influence of the parallel electric field while the right column (a_2, b_2, c_2, and d_2) shows the cones under the influence of the perpendicular field. The solid lines represent the situation where there is no external electric field, the dashed ones refer to the 0.30 V/Å situation, and finally, the pointed lines show the densities of states when the cones are submitted to electric fields equal to 0.50 V/Å. One can observe the great difference between the parallel and perpendicular situation for the cones with 60° (both B–B and N–N) and 120° disclination (a_1 and a_2, b_1 and b_2, and c_1 and c_2). For the first case (a_1, b_1, and c_1) we have little influence of the field at the states around Fermi Energy (E_F), however, when the direction of the field is changed, becoming perpendicular (a_2, b_2, and c_2), there is a gap reduction of about 1.16 eV (1.3 eV) when the field is equal to 0.30 V/Å and to 2.9 eV (2.6 eV) when it is equal to 0.50 V/Å for the 60° B–B (N–N) cone. For the 120° there is a gap reduction of about 1.5 eV when the field is equal to 0.30 V/Å and to 2.7 eV when it is equal to 0.50 V/Å. The 240° cone, however, presents a unique behavior where both directions of the electric field generate a gap closure that is 0.27 eV (1.7 eV) for the parallel case, 0.65 eV (1.15 eV) for the perpendicular case with 0.30 V/Å (0.50 V/Å), respectively. Figure 3(c) illustrates this behavior where we have a crossing point showing that for electric-field magnitudes higher than ≈0.38 V/Å, the parallel direction closes the energy gap in a more effective way for this disclination angle. This gap reduction (observed for a_2, b_2, c_2, d_1, and d_2) would lead to a reduction of the work function of the BN nanocones that, by its turn, increases the field-emission properties of these systems.

TABLE I. Formation energies for the cones with 120° and 240° disclination under the influence of different magnitudes of the external electric field (from 0.0 to 0.50 V/Å) applied in a direction perpendicular and parallel to the cones' axis.

	120°		240°	
	Perpendicular	parallel	Perpendicular	parallel
ε(V/Å)	E_f(eV)/n_{BN}	E_f(eV)/n_{BN}	E_f(eV)/n_{BN}	E_f(eV)/n_{BN}
0.00	0.14	0.14	0.32	0.32
0.05	0.14	0.14	0.31	0.32
0.10	0.14	0.14	0.31	0.31
0.20				0.31
0.30	0.13	0.14	0.30	0.31
0.50	0.11	0.13	0.28	0.26

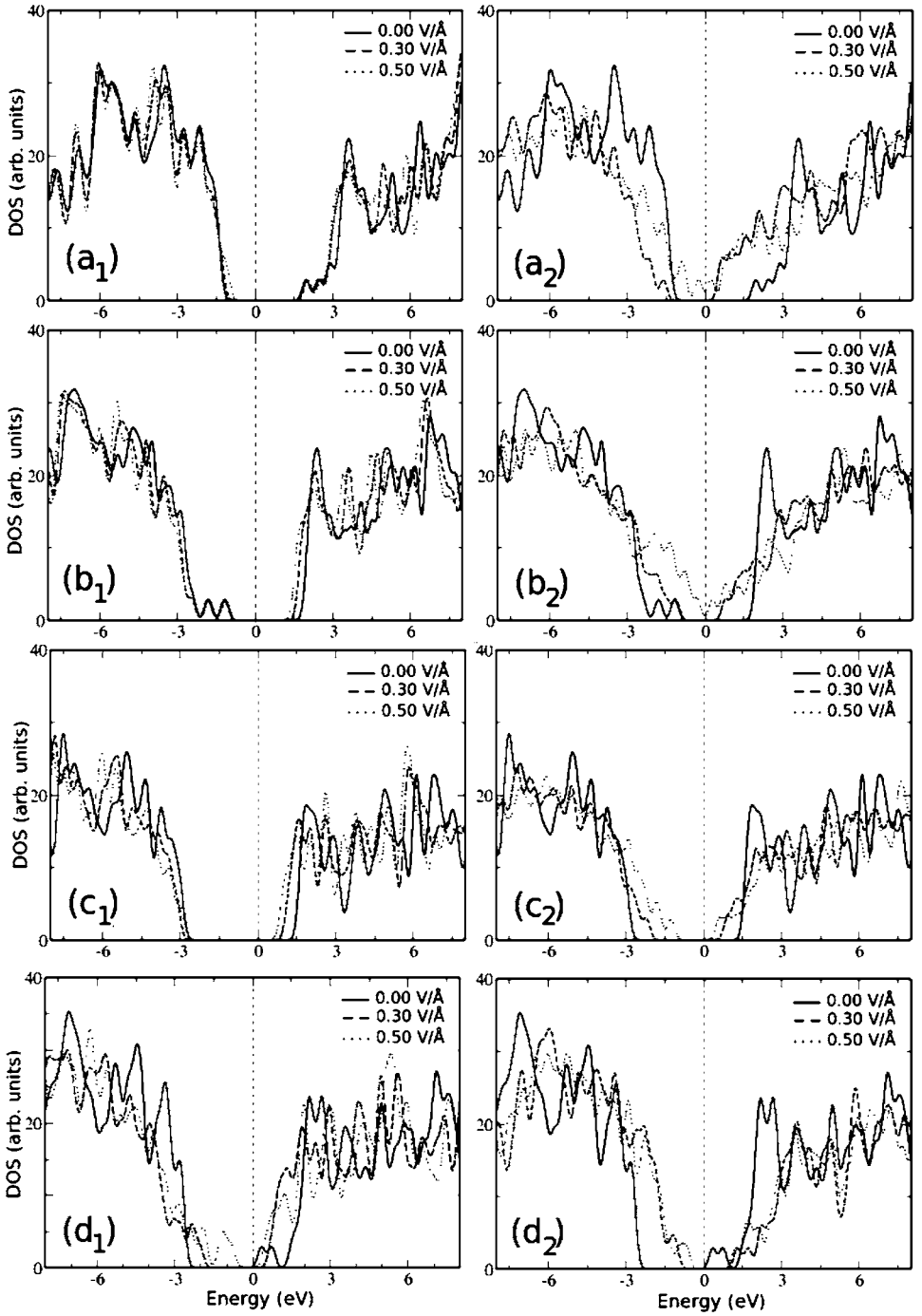

FIG. 2. Densities of states for the cones with (a) 60° B–B, (b) 60° N–N, (c) 120°, and (d) 240° disclination under the influence of parallel (left column, index 1) and perpendicular (right column, index 2) external electric fields. The solid, dashed, and pointed lines correspond to the 0.00, 0.30, and 0.50 V/Å, respectively.

The behavior of the densities of states of the cones can be better understood when we compare our results with the ones obtained for BN nanotubes under the influence of perpendicular electric fields.[19] It was observed that a Stark effect takes part at the gap closure by mixing the nearby subband states separately in both valence and conduction bands for small values of applied electric fields. According to that work we could expect to see the reduction of the gap for the 60° and 120° cones for higher values of the parallel electric field (situation a_1, b_1, and c_1). It was also shown that the charge-density corresponding to the bottom of the conduction band is highly localized at one side of the tube while the top of the valence band is localized at the other. The same occurs for our cones when they are under the influence of the perpendicular electric field (see Fig. 5). Finally, it was observed that the larger the diameter of the nanotube the larger would be the gap reduction for a given magnitude of the applied electric field. This is also true for our cones when we make a comparison between the homonuclear-defect-free cones (120° and 240°) where we can see a higher gap reduction for the first one which presents a larger "open edge diameter" (smaller disclination angle) when compared with the second one. In fact, if we take a closer look at Figs. 3(a) and 3(b) we can see a quadratic behavior for both the 60° and 120° disclination cones, that is again associated with the Stark effect observed previously for BN nanotubes. In that

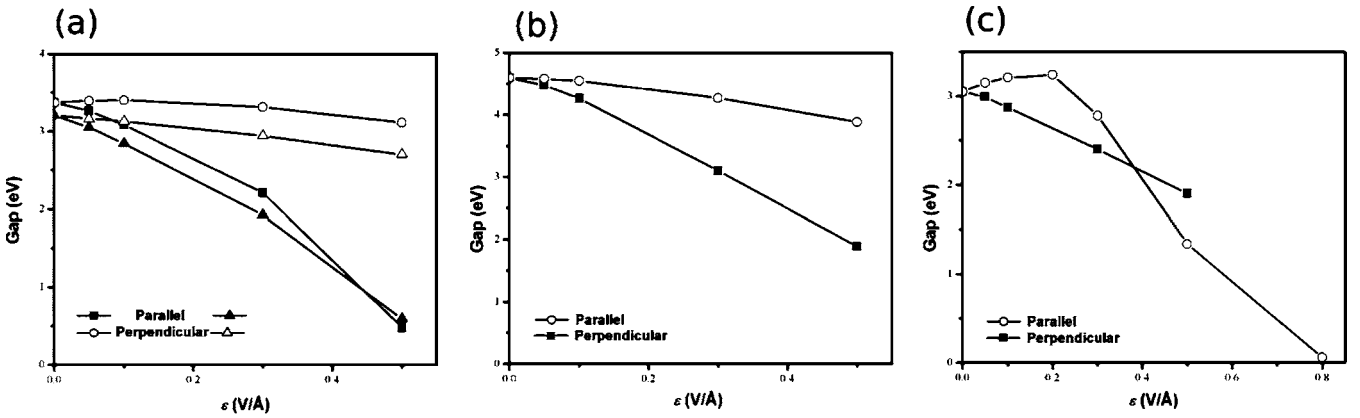

FIG. 3. Variation of the gap associated with the magnitude of the external electric field, applied parallelly (circle) and perpendicularly (square), for the systems (a) 60° B–B and N–N (represented here by triangles), (b) 120°, and (c) 240°.

way we can say that there is rule for tuning the gap of boron-nitride nanocones through the application of an external electric field: for smaller disclination angles one would be more efficient by applying a perpendicular electric field, while for larger ones a parallel electric field is better. Indeed we extrapolate this rule as trying to foresee the magnitude of the external electric field, either parallel or perpendicular, needed to completely close the energy gap that are (i) for the 60° B–B (N–N) cone: 1.51 (1.76) and 0.54 (0.57) V/Å for the parallel and perpendicular fields, respectively (the N–N one having a very similar behavior), and (ii) for the 120° cone: 1.44 and 0.74 V/Å for the parallel and perpendicular fields, respectively. Furthermore, the magnitude of the electric field applied perpendicularly to the 240° cone that is strong enough to completely close the energy gap is ≈1.09 V/Å while the calculated value for doing this closure, when the field is parallel, is ≈0.8 V/Å.

The next discussion is about the energy shift, as function of the external electric field as showed in Fig. 4. The calculations are done according to the equation:

$$\Delta E = E - E_0, \tag{3}$$

where E (E_0) is the total energy with (without) the presence of the external electric field. The energy shift, that is a perturbation caused by the external electric field, which, by its turn causes the splitting of energy levels, can be well fitted by a quadratic function of the applied field (ε) being $\Delta E = -8.13\varepsilon^2 - 0.34\varepsilon - 0.02$ for the 60° B–B disclination cone, $\Delta E = -9.18\varepsilon^2 + 0.18\varepsilon$ for the 60° N–N disclination cone, $\Delta E = -6.97\varepsilon^2 - 0.49\varepsilon - 0.02$ for the 120° one and $\Delta E = -5.74\varepsilon^2 - 1.77\varepsilon$ for the 240° cone when the field is perpendicularly applied and $\Delta E = -3.70\varepsilon^2 - 0.65\varepsilon$ for the 60° B–B disclination cone, $\Delta E = -4.16\varepsilon^2 + 1.29\varepsilon + 0.02$ for the 60° N–N disclination cone $\Delta E = -3.77\varepsilon^2 - 1.03\varepsilon$ for the 120° one, and $\Delta E = -8.54\varepsilon^2 + 1.52\varepsilon - 0.02$ for the 240° cone when the field is parallel to the cones' axis. This quadratic function demonstrates the occurrence of second-order Stark effect as predicted by An *et al.*[31] It can be easily seen, from both the results shown above and in Fig. 4, the more pronounced quadratic character for the situation where the field is perpendicularly applied (except for the 240° case). This effect emphasizes the results obtained for the densities of states [see Fig. 3] that already showed the influence of perpendicular electric fields at cones with disclination angles smaller than 240°, i.e., with larger open edge diameters.

In Fig. 5 we can see the electronic densities at the top of the valence and bottom of conduction band for the cones 120° (left) and 240° (right). At first we can observe the great difference for the parallel [top, (a_1) and (a_2))] and perpendicular [bottom, (a_3) and (a_4)] field situation, with magnitude equal to 0.5 V/Å, for the 120° cone. While for the first

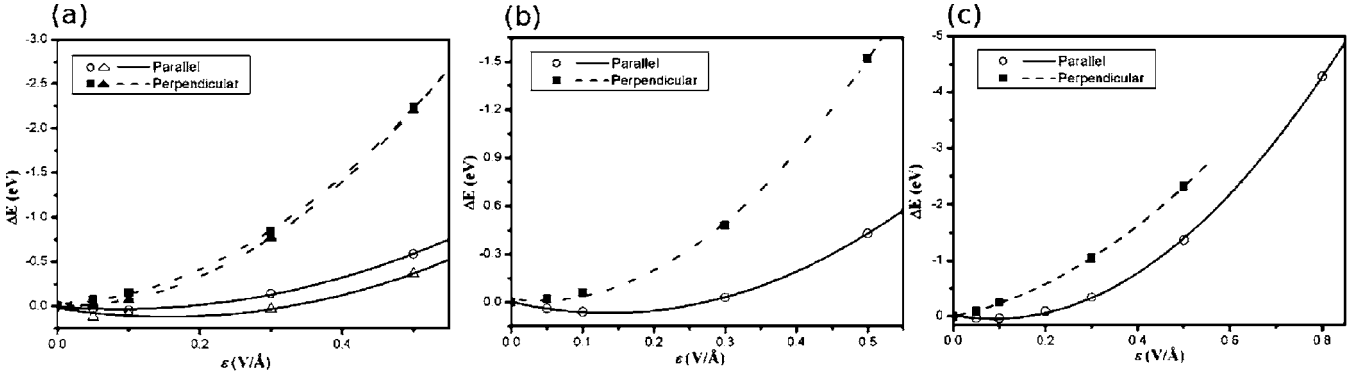

FIG. 4. Energy shift for the cones (a) 60° B–B and N–N (represented by triangles), (b) 120° and (c) 240° under the influence of external electric fields either parallel (circle) or perpendicular (square) to the cones' axis.

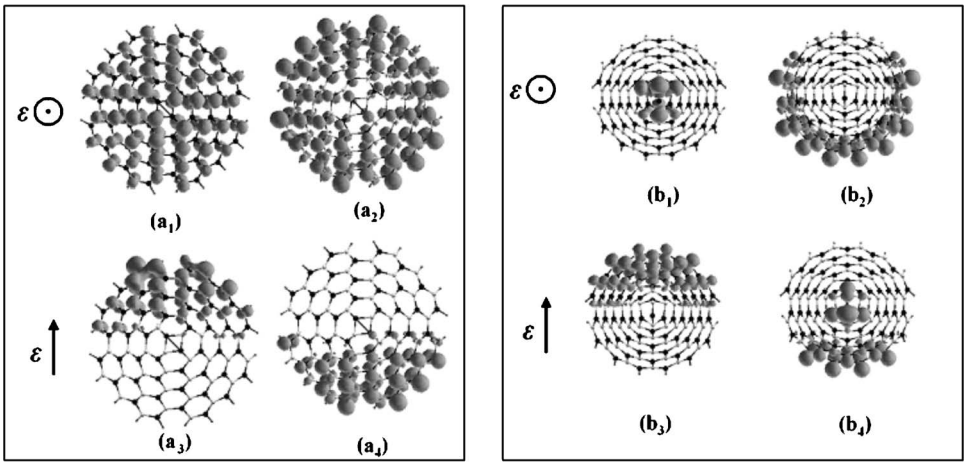

FIG. 5. Electronic densities for the 120° cone being (a_1) and (a_2) $[(a_3)$ and $(a_4)]$, the top of valence and bottom of conduction bands, respectively, for the field equal to 0.5 V/Å applied parallell (perpendicular) to the cone axis; 240° cone being (b_1) and (b_2) $[(b_3)$ and $(b_4)]$ the top of valence and bottom of conduction bands, respectively, for the field equal to 0.5 V/Å applied parallell (perpendicular) to the cone axis. The B (N) atoms are represented by black (white) dots.

case $[(a_1)$ and $(a_2)]$ we see a regular distribution of the electronic density either at valence or conduction band, for the second one $[(a_3)$ and $(a_4)]$ we have a polarization of those bands with the electronic density at the top of the valence band moved toward the electric-field direction and the electronic density corresponding to the bottom of conduction band moved in the direction opposite to the electric field. We can also observe from the figure that the charge tends to accumulate at the N atoms [represented by white dots in Fig. 5] with the application of the field, which is related with nitrogen atoms' larger electronegativity. Similar results were obtained for perpendicular electric field applied to BN nanotubes by Khoo *et al.*[19] The results for the 60° disclination cone are very similar to the ones for the 120° one, the main difference being the presence of the line of homonuclear B–B and N–N bonds for the 60° ones. These lines of homonuclear bonds tend to concentrate charge. Finally, for the 240° disclination cone we have the situation shown in the figure $[(b_1)$, (b_2), (b_3), and $(b_4)]$. When the field is applied parallelly to the cone axis we have a electronic density concentration, for the top of the valence band, at the tip of the cone (b_1) together with the localization of the bottom of the conduction band at the base of the cone (b_2), and not the homogeneous distribution that we see for the 120° cone. This behavior can be strictly related to the higher curvature of the 240° disclination cone when compared to the other cones. Indeed, even when the electric field is applied perpendicularly and the polarization as seen for the 120° cone arises, we can still see the density concentration, for the bottom of the conduction band, at the tip of the 240° disclination cone.

In summary, we have done first-principles calculations on BN nanocones under the influence of external electric fields either parallel or perpendicular to the cones' axis with magnitudes ranging from 0 to 0.5 V/Å. The results showed that there is little field influence at the formation energy of the cones that reinforces the idea of those structures having good geometrical stability. For the densities of states we have seen that there is a relationship between the cones disclination angle with their response to the direction of the applied field: for smaller disclination angles one would be more efficient by applying a perpendicular electric field, while for larger ones a parallel electric field is better when tuning the gap of those structures. A second-order Stark effect is observed when we analyze the energy shift for the cones under the influence of electric fields. The last results can be related to previous ones for BN nanotubes where it was observed that a Stark effect takes part at the gap closure of those structures.[19] Our results show that different electronic properties are related with different disclination angles of the cones and provide a path to be followed by experimentalists when trying to tune the gap of BN nanocones through the application of electric fields.

ACKNOWLEDGMENTS

This work was supported by the Brazilian Agencies FAPESB and CNPq.

[1] H. W. Kroto, J. R. Heath, S. C. O'Brien, R. F. Curl, and R. E. Smalley, Nature (London) **318**, 162 (1985).
[2] S. Iijima, Nature (London) **354**, 56 (1991).
[3] N. Hamada, S. I. Sawada, and A. Oshiyama, Phys. Rev. Lett. **68**, 1579 (1992).
[4] S. Iijima, T. Ichihashi, and Y. Ando, Nature (London) **356**, 776 (1992).
[5] M. Ge and K. Sattler, Appl. Phys. Lett. **64**, 710 (1994).
[6] M. Ge and K. Sattler, Chem. Phys. Lett. **220**, 192 (1994).
[7] L. R. Baylor, V. I. Merkulov, E. D. Ellis, M. A. Guillorn, D. H. Lowndes, A. V. Melechko, M. L. Simpson, and J. H. Whealton, J. Appl. Phys. **91**, 4602 (2002).
[8] K. A. Dean and B. R. Chamala, J. Appl. Phys. **85**, 3832 (1999).
[9] Y. Chen, J. Zou, S. J. Campbell, and G. Le Caer, Appl. Phys. Lett. **84**, 2430 (2004).
[10] R. Z. Ma, D. Golberg, Y. Bando, and T. Sasaki, Philos. Trans. R. Soc. London, Ser. A **362**, 2161 (2004).
[11] S. Azevedo, M. S. C. Mazzoni, H. Chacham, and R. W. Nunes, Appl. Phys. Lett. **82**, 2323 (2003).
[12] S. Azevedo, M. S. C. Mazzoni, R. W. Nunes, and H. Chacham,

Phys. Rev. B **70**, 205412 (2004).
[13] C. Zhi, Y. Bando, C. Tang, and D. Golberg, Phys. Rev. B **72**, 245419 (2005).
[14] L. Bourgeois, Y. Bando, W. Q. Han, and T. Sato, Phys. Rev. B **61**, 7686 (2000).
[15] D. Golberg, A. Rode, Y. Bando, M. Mitome, E. Gamaly, and B. Luther-Davies, Diamond Relat. Mater. **12**, 1269 (2003).
[16] T. Oku, A. Nishiwaki, and A. Narita, Sci. Technol. Adv. Mater. **5**, 635 (2004).
[17] C. Zhi, Y. Bando, C. Tang, and D. Golberg, Appl. Phys. Lett. **87**, 063107 (2005).
[18] J. Cumings and A. Zettl, Solid State Commun. **129**, 661 (2004).
[19] K. H. Khoo, M. S. C. Mazzoni, and Steven G. Louie, Phys. Rev. B **69**, 201401(R) (2004).
[20] S. Azevedo and F. de B. Mota, Int. J. Quantum Chem. **106**, 1907 (2006).
[21] S. Azevedo, M. S. C. Mazzoni, H. Chacham, and R. W. Nunes, Appl. Phys. Lett. **82**, 2323 (2003).
[22] M. Machado, P. Piquini, and R. Mota, Nanotechnology **16**, 302 (2005).
[23] M. Machado, P. Piquini, and R. Mota, Chem. Phys. Lett. **392**, 428 (2004).
[24] W. Kohn and L. J. Sham, Phys. Rev. **140**, A1133 (1965).
[25] J. P. Perdew, K. Burke, and M. Ernzerhof, Phys. Rev. Lett. **77**, 3865 (1996).
[26] D. Sanchez-Portal, P. Ordejon, E. Artacho, and J. M. Soler, Int. J. Quantum Chem. **65**, 453 (1997).
[27] O. F. Sankey and D. J. Niklewski, Phys. Rev. B **40**, 3979 (1989).
[28] E. Artacho, D. Sanchez-Portal, P. Ordejon, A. Garcia, and J. M. Soler, Phys. Status Solidi B **215**, 809 (1999), and references therein.
[29] N. Troullier and J. L. Martins, Phys. Rev. B **43**, 1993 (1991).
[30] L. Kleinman and D. M. Bylander, Phys. Rev. Lett. **48**, 1425 (1982).
[31] W. An, W. Xiaojun, and X. C. Zeng, J. Phys. Chem. B **110**, 16346 (2006).